Short communication

# Inverse vulcanization of all-*cis*-fluorinated cyclohexylacrylate: Tailored polymers for Li-S battery cathode materials☆

Alexander P. Grimm [a] 🔵, Bijian Deng [b], Shyamkumar V. Haridas [c], Dominik Voll [d],
Christian W. Schmitt [a], Max von Delius [c], Frieder Scheiba [b], Patrick Théato [a,d,*]

[a] *Institute for Biological Interfaces III (IBG-3), Soft Matter Synthesis Laboratory, Karlsruhe Institute of Technology (KIT), Hermann-von-Helmholtz-Platz 1, 76344 Eggenstein-Leopoldshafen, Germany*
[b] *Institute for Applied Materials – Energy Storage Systems (IAM-ESS), Karlsruhe Institute of Technology (KIT), Hermann-von-Helmholtz-Platz 1, 76344 Eggenstein-Leopoldshafen, Germany*
[c] *Institute of Organic Chemistry, University of Ulm, Albert-Einstein-Allee 11, 89081 Ulm, Germany*
[d] *Institute for Technical Chemistry and Polymer Chemistry (ITCP), Karlsruhe Institute of Technology (KIT), Engesserstraße 18, 76131 Karlsruhe, Germany*

ABSTRACT

The use of elemental sulfur as an alternative feedstock for polymer synthesis by inverse vulcanization has shown to be an elegant, yet simple way towards materials with high sulfur contents. Besides, their use as fertilizers, optical lenses, and heavy metal sorbents, those materials are considered as next generation cathode materials for lithium-sulfur batteries with exceptionally high specific capacities. However, Li-S battery cathodes typically exhibit a rapid capacity fading caused by a phenomenon called 'polysulfide shuttle-effect'. Herein, we report the synthesis of a terpolymer comprised of all-*cis*-fluorinated cyclohexyl acrylate and triethoxyvinylsilane via inverse vulcanization in *N*-methyl-2-pyrrolidone at 150 °C with subsequent silane polycondensation to obtain stable Li-S battery cathodes with sulfur contents of 61 wt%. Electrochemical analysis of Li-S cells showed higher lithium-ion diffusion, superior cycling capacity retention (98 % after 200 cycles at 1C), and suppressed self-discharge (0.02 V after 21 days) compared to the non-fluorinated reference material (38 % capacity retention after 200 cycles at 1C and 0.07 V self-discharge after 21 days). The highly polar nature of fluorinated cyclohexane moieties is believed to significantly inhibit the 'polysulfide shuttle-effect', by coordination of polysulfides.

## 1. Introduction

Despite its established role in the vulcanization of polydienes, the broader use of elemental sulfur in materials science has been relatively unexplored and only experienced an upswing in recent years. Currently, around 70 million tons of elemental sulfur are produced annually, mostly as a byproduct of oil refining, natural gas processing, or coking via the Claus process. [1] The vast availability and low cost of sulfur encouraged its use as a sustainable and cost-effective feedstock for functional materials. [2,3] In the past years, sulfur-based copolymeric materials have emerged, primarily driven by the pioneering work of Pyun's group. Initially, Pyun and colleagues converted elemental sulfur with 1,3-diisopropenylbenzene (DIB) by simple mixing at temperatures up to 185 °C, producing hyperbranched copolymers with sulfur contents

of up to 95 wt%. [4] This process, known as "inverse vulcanization" (IV), involves converting elemental sulfur with unsaturated organic co-monomers to create chemically stable polymeric materials with high sulfur content (> 50 wt%). [5] IV is an economical, and solvent-free synthesis method with applications in various fields including heavy metal sorbents, [6,7] infrared optics, [8,9] antibacterial surfaces, [10] thermal insulators, [11] fertilizers, [12,13] and healable materials. [14,15] Importantly, inverse vulcanized copolymers have found applications as cathode materials in lithium-sulfur (Li-S) batteries. [4,16,17] Li-S batteries are particularly promising for meeting the growing demand for high-capacity energy storage systems due to their low toxicity, cost-effectiveness, and abundance of active materials. Compared to conventional Li-ion batteries, which use heavy metal oxides as cathode materials, Li-S batteries offer ten times higher theoretical capacity and

five times higher specific energy density. [18] However, so far most Li-S batteries suffer from short cycle lifetimes, self-discharge and, most importantly, polysulfide shuttling. These issues are often attributed to the dissolution of long-chain polysulfides and the low conductivity of sulfur. [19].

Among the various strategies to address these problems, sulfur co-polymers have recently attracted significant attention due to their simple synthesis, which have shown to improve the cycling stability and specific capacities of Li-S batteries. This enhanced cyclability is thought to result from better compatibility with conductive carbon and improved mechanical stability of the cathode materials, although the exact mechanisms behind the improved performance are not fully understood. [20] In order to address the issue of polysulfide shuttling, confinement of soluble poly-, and oligosulfides is necessary to reduce the loss of capacity during cell cycling. Molecules that can bind to anions and specifically sulfides through supramolecular interactions are highly interesting candidates in this scenario. Yet, such molecules must also provide a sufficient electrochemical stability to find application within a battery. A promising emerging chemical motif that has been shown to be able to bind anions via hydrogen bond coordination are all-*cis*-1,2,3,4,5,6-hexafluoro cyclohexane derivatives. [21,22] This molecule has first been reported in 2015 by O'Hagan and coworkers, [23] and applications in anion sensing,[24] medicinal chemistry, [25] liquid crystals, [26] and supramolecular polymerization have since been reported. [27–29] We hypothesize, that the presence of these high-polar moieties would inhibit the polysulfide shuttling and result in an improved capacity retention of Li-S batteries compared to an analogous non-high-polar cathode material (refer to SI, Fig. S1). Herein, we report for the first time the synthesis of all-*cis*-2,3,4,5,6-pentafluorocyclohexyl acrylate (PFCHA) along with its IV and application as cathode material in Li-S battery cathodes.

The PFCHA monomer was synthesized following the methodology established by Glorius [30] via a three-step synthesis (refer to SI, Scheme S1). Pentafluoroanisol was selectively all-*cis*-hydrogenated with pressurized hydrogen gas under presence of the rhodium catalyst [Rh(CAAC)(COD)Cl]. The obtained, so-called, 'Janus-faced' (i.e. two-faced) all-*cis*-fluorinated methoxy derivative was deprotected to obtain all-*cis*-2,3,4,5,6-pentafluorocyclohexyl alcohol. [28] All-*cis*-2,3,4,5,6-pentafluorocyclohexyl alcohol was then acrylated by reaction with acryloyl chloride in the presence of 2,6-lutidine. The successful synthesis of PFCHA was confirmed by nuclear magnetic resonance (NMR)

spectroscopy and mass spectrometry (refer to SI, Figs. S2 – S4). The proposed Li-S battery cathode materials reported in this work were obtained via IV of PFCHA in presence of triethoxyvinylsilane (TEVS) in *N*-methyl-2-pyrrolidone (NMP) at 150 °C for 18 h with subsequent silane hydrolysis and polycondensation (for detailed procedure, refer to SI). IV of PFCHA without TEVS yielded a material that was readily soluble in THF and NMP and was therefore not applicable as cathode material in liquid electrolyte-based batteries. Therefore, TEVS was added to the formulation as cross-linking agent, which would provide insolubility of the cathode material via siloxane formation upon a subsequent polycondensation (refer to SI, Fig. S5a – d). The non-polar reference material was prepared analogously under substitution of PFCHA with cyclohexyl acrylate (CHA) (refer to Scheme 1). The ratio of S:PFCHA/CHA:TEVS was set to 50:25:25 wt%, motivated by the balance between electrochemical capacity (stemming from S), number of binding sites (provided by PFCHA), and insolubility (from TEVS). The resulting materials were named poly(sulfur-all-*cis*-2,3,4,5,6-pentafluorocyclohexylacrylate-triethoxyvinylsiloxane) (poly(S-PFCHA-TEVS)) and poly(sulfur-cyclohexylacrylate-triethoxyvinylsiloxane) (poly(S-CHA-TEVS)), respectively. In the following, poly(S-PFCHA-TEVS) refers to the polymer with the composition S:PFCHA/CHA:TEVS of 50:25:25 wt%. Deviating polymer compositions are indicated by subscript weight ratios. Reduction of TEVS content to 15 wt% yielded poly($S_{60}$-PFCHA$_{25}$-TEVS$_{15}$) which was found to still be slightly soluble in the electrolyte solution of dimethoxyethane/1,3-dioxolane (DME/DOL) (1:1 v/v) (refer to SI, Fig. S5e). Despite the avoidance of transition metal accelerators during the IV, no formation of $H_2S$ gas was observed. Full conversion of elemental sulfur into organic polysulfides was confirmed by differential scanning calorimetry (DSC), as the DSC traces showed no melting of crystalline sulfur in the range of 110 – 120 °C for both poly(S-PFCHA-TEVS) and poly(S-CHA-TEVS) (refer to Fig. 1A). However, increasing the sulfur content of the polymer to 60 wt%, resulted in the presence of residual crystalline sulfur in poly($S_{60}$-PFCHA$_{25}$-TEVS$_{15}$) as has been found by DSC analysis, limiting the sulfur content to 50 wt% (refer to SI, Fig. S6a). Interestingly, poly(S-PFCHA-TEVS) showed no clearly distinguishable glass transition in the investigated temperature range between −25 °C and 150 °C at a heating rate of 10 K min$^{-1}$ while poly(S-CHA-TEVS) exhibited a glass transition temperature at 25 °C which shifted to 5 °C in the second heat run. Increasing the heating rate to 20 K min$^{-1}$ however, allowed an estimation of the $T_g$ at 138 °C for poly(S-PFCHA-TEVS) (refer to SI, Fig. S6b). This can be explained by the strong
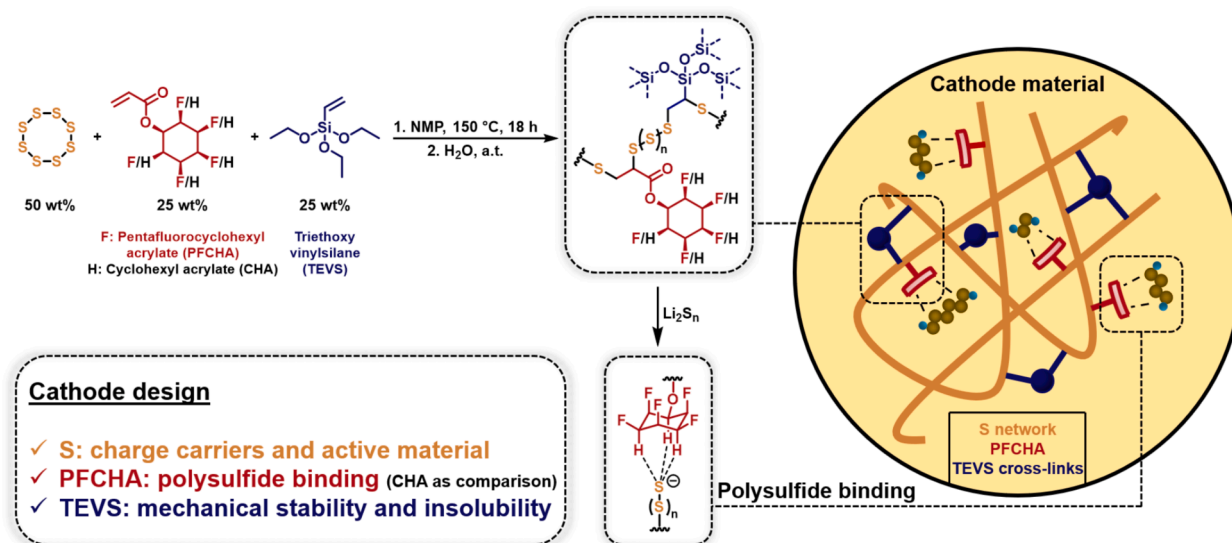


**Scheme 1.** Reaction scheme of the inverse vulcanization of both pentafluorinated (red) and non-fluorinated (black) cyclohexyl acrylate with triethoxyvinylsilane (left). Silane hydrolysis and condensation yields insoluble cathode materials with modulated polarity, which facilitates coordination of polysulfides and therefore hinders polysulfide shuttling in the cathode material (right).
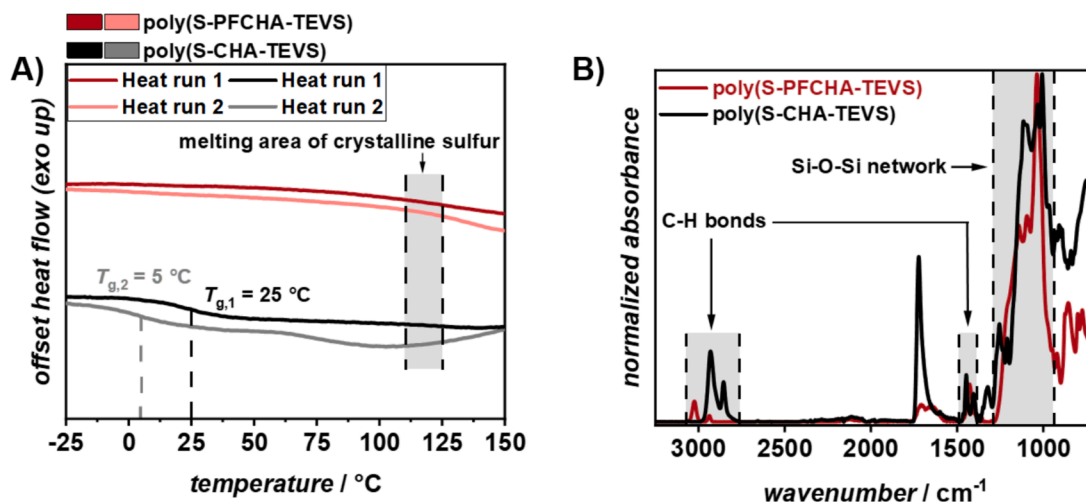
**Fig. 1.** DSC thermograms (A) and FT-IR spectra (B) of poly(S-PFCHA-TEVS) (red) and poly(S-CHA-TEVS) (black).The DSC thermograms show no melting of residual crystalline sulfur in the region of 110 – 120 °C, confirming full conversion of elemental sulfur during the IV. FT-IR spectra show the presence of C–H and Si-O-Si network bond vibrations under absence of characteristic C = C double bond vibrations, indicating full conversion of TEVS, and PFCHA and CHA, respectively.

interaction between the two "Janus" faces of the fluorinated cyclohexyl rings, which hinders thermal chain movement and therefore influences the $T_g$ compared to the non-fluorinated material.[23,31] Attenuated total reflection Fourier-transformation infrared (ATR FT-IR)

spectroscopy showed the presence of a very strong and broad absorption band in the region of 1250 – 900 cm$^{-1}$, which indicated the formation of Si-O-Si networks by polycondensation of TEVS. [32] Additionally, the absence of characteristic vinyl C–H and C = C bond vibrations at 3080
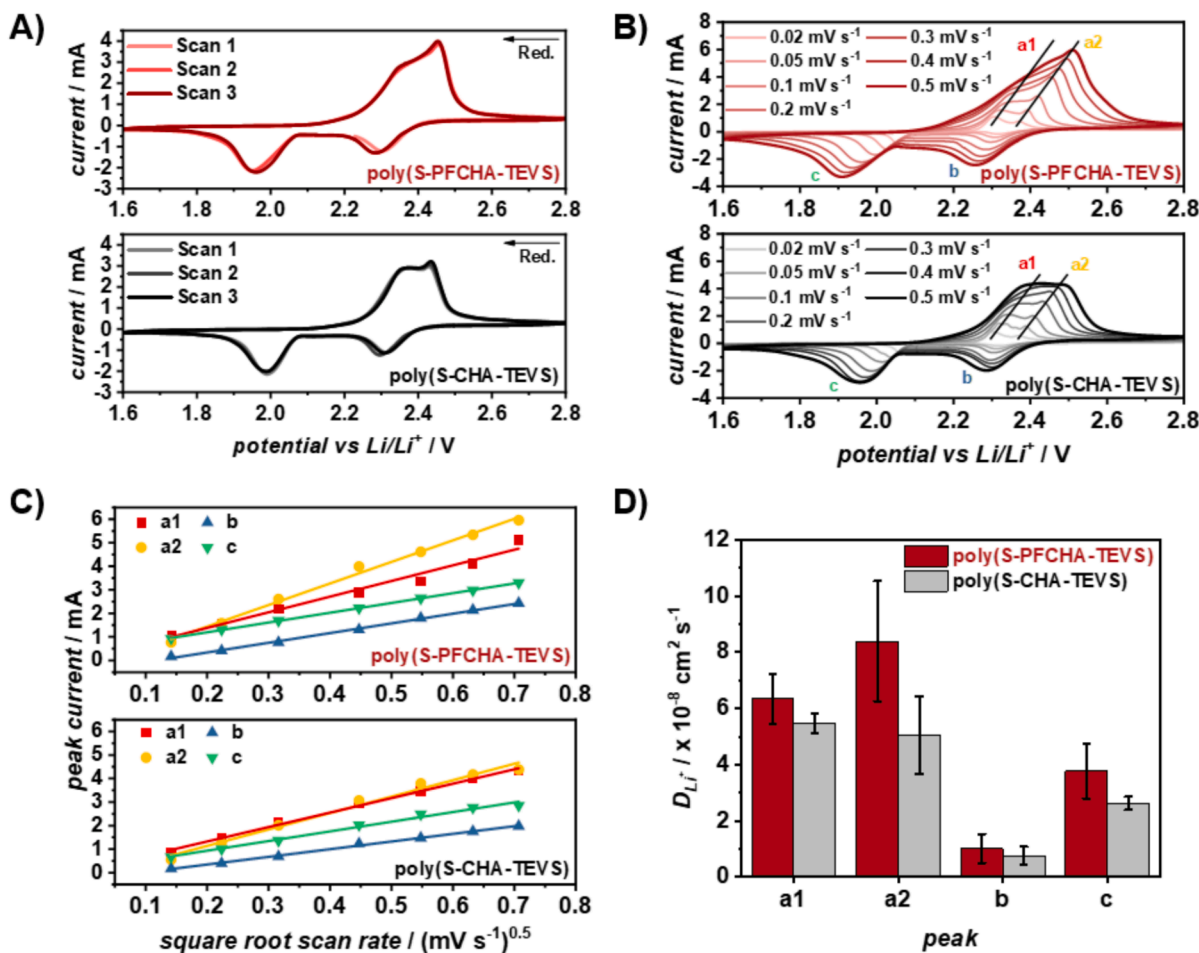


**Fig. 2.** Cyclic voltammetry analysis of poly(S-PFCHA) (red) and poly(S-CHA-TEVS) (black) against lithium. A) CV plots of both materials at constant scan rate ($\nu =$ 0.2 mV s$^{-1}$) for three cycles, showing stable redox behavior. B) Scan rate sweeps of both materials from 0.02 – 0.5 mV s$^{-1}$. The increase in current with the scan rate was used to calculate the lithium-ion diffusion coefficient according to the Randles-Ševčík equation (C-D).

and 900 cm$^{-1}$, respectively, was indicative to the successful conversion of comonomer double bonds during the IV with elemental sulfur under the chosen reaction conditions (refer to Fig. 1B). Elemental analysis of poly(S-CHA-TEVS) revealed a sulfur content of 61 wt%, which was in accordance with the theoretical sulfur content (57 wt%, after elimination of ethanol due to polycondensation). To validate the sulfur contents of both materials, thermogravimetric analysis (TGA) was conducted. The thermograms of poly(S-PFCHA-TEVS) and poly(S-CHA-TEVS) show one thermal degradation occurring at 180 °C which accounts for a weight loss of around 60 wt% and can be associated with the decomposition of polysulfide species in the material (refer to SI, Fig. S7). The remaining weight after thermal decomposition can be explained by silica networks from cross-linked TEVS residues, which are known to be thermally stable up to over 1000 °C. [33].

Li-S cells with both poly(S-PFCHA-TEVS) and poly(S-CHA-TEVS) as cathode materials were fabricated and subjected to cyclic voltammetry (CV) to evaluate their electrochemical activity (for cell fabrication and electrochemical test procedures, refer to SI). During the first cycle, two cathodic peaks were observed at 2.30 V and 1.95 V for poly(S-PFCHA-TEVS) and at 2.30 V and 1.99 V for poly(S-CHA-TEVS), respectively, showing no significant shift of the redox potential with change of the acrylate. These peaks are characteristic of the stepwise reduction of elemental sulfur in liquid electrolyte Li–S batteries (refer to Fig. 2A). [34] The peak at 2.30 V was attributed to the reduction of polysulfide chains, resulting in the formation of high-order inorganic polysulfides (Li$_2$S$_x$, where x $= 6 - 8$) and high-order organic polysulfides bonded to PFCHA and TEVS (C–S$_x$–Li, where x $= 6 - 8$). At approximately 1.95 V and 1.97 V, respectively, these high-order polysulfides were further reduced to low-order inorganic polysulfides (Li$_2$S$_x$, where x $= 1 - 3$) and low-order organic polysulfides (C–S$_x$–Li, where x $= 1 - 3$). [35] During the reverse process, a split broad anodic peak with maxima at 2.36 V and 2.45 V for both materials was attributed to the oxidation of the low-order lithium polysulfides to high-order lithium polysulfides (refer to SI, Scheme S1). [36]The overall slightly larger peak area of the cyclic voltammogram of poly(S-PFCHA-TEVS), mainly from the second oxidation and the first reduction peak, further indicates promoted polysulfide conversion by improved Li$^+$ ion mobility. [37] The well-maintained cathodic and anodic peaks throughout the three cycles indicated the thorough reversibility of the electrochemical reaction.

To uncover the variations in the apparent diffusion coefficient of lithium ions ($D_{Li}^+$), additional cyclic voltammetry measurements were performed at varying sweep rates (refer to Fig. 2B). The cathodic and anodic peak currents demonstrated a linear relationship with the square root of the scan rate, consistent with the Randles-Sevcik equation (refer to Fig. 2C), which correlates the slope of the curve ($I_p$ $\nu^{-0.5}$) to the apparent $D_{Li}^+$ for the specific electrochemical step:

$$I_p = \left(2.69 \times 10^5\right) n^{1.5} A C_{Li} \sqrt{D_{Li^+} \nu}$$

$I_p$ is the peak current of the individual redox peak (A), $n$ is the number of charge transferred during a redox step ($= 1$), $A$ is the electrode area (cm$^2$), $C_{Li}$ represents the concentration of lithium ions in the system (mol cm$^{-3}$), $\nu$ is the scan rate (V s$^{-1}$), and $D_{Li}^+$ is the diffusion coefficient of lithium ions (cm$^2$ s$^{-1}$). [38] The lithium diffusion coefficients for both materials are displayed in Fig. 2D and the supporting information (refer to SI, Table S1 and S2). It is apparent that $D_{Li}^+$ was significantly higher for the material that contains high-polar PFCHA moieties which substantiates the hypothesis of improved Li$^+$ diffusion by confinement of sulfides at the coordinating sites in the cathodes which reduces viscosity of the electrolyte and therefore the lithium diffusion. [38] However, it needs to be noted that the exact underlying mechanism remains not fully understood and unveiling the location of binding effects occurring in bulk or at the interfaces needs to be further investigated in future studies.

The electrochemical charge–discharge cycling performance of poly(S-PFCHA-TEVS) and poly(S-CHA-TEVS) against lithium metal was studied by long-term cycling at 1C (refer to Fig. 3A and SI, Fig. S8A). Interestingly, the initial capacity of around 550 mAh g$^{-1}$ of poly(S-CHA-TEVS) was found to quickly fade to around 280 mAh g$^{-1}$ in the first 50 cycles ($\approx$ 51 % retention). This initial capacity loss was due to the irreversible loss of soluble polysulfide species and the deposition of polysulfides and decomposed electrolyte components on the lithium metal anode with a total capacity retention of 38 % after 200 cycles. On the contrary, poly(S-PFCHA-TEVS) showed no such initial loss of capacity. Furthermore, the capacity was found to increase by approximately 12 % from 550 mAh g$^{-1}$ to 650 mAh g$^{-1}$ in the first 100 cycles, before slowly decaying. After 200 cycles, the initial capacity of 550 mAh g$^{-1}$ was met. After 400 cycles the cells failed at a residual capacity of 150 mAh g$^{-1}$ which represents approximately 27 % of the original capacity. Additional long-term cycle at 0.5C has been conducted which showed an increased overall capacity for both cathode materials as expected by the rate-capacity effect (refer to SI, Fig. S8B). Cells containing CHA showed a steep capacity loss of 29 % during the first 10 cycles which was not observed for PFCHA containing cells. After 500 cycles, a capacity of 543 mAh g$^{-1}$ was met which resembles an overall capacity retention of 63 %. Cells containing poly(S-PFCHA-TEVS) cycled at 0.5C showed a less smooth capacity trend but were found to still exhibit 96 % of their initial capacity after 200 cycles before capacity fading set in. After 500 cycles at 0.5C, a capacity of 391 mAh g$^{-1}$ (44 %) was retained. While the reason for the increase in capacity and the good capacity retention despite the low Coulombic efficiency is currently unclear, the integration of all-*cis*-fluorinated cyclohexyl groups into the cathode material is evidently beneficial on the cycling performance. Electrochemical impedance spectroscopy (EIS) was performed of Li-S cells with poly(S-PFCHA-TEVS) and poly(S-CHA-TEVS), respectively after 100 and 200 cycles (refer to SI, Fig. S9) to uncover charge transfer processes at the electrode/electrolyte interface. Interestingly, cells containing poly(S-PFCHA-TEVS) as cathode material showed no increase in impedance over 100 additional cycles which is in line with the long-term cycling performance. In contrast, the impedance of CHA-containing cells increased slightly from cycle number 100 to 200. This can be explained by the formation of a Li$_2$S/Li$_2$S$_2$ layer on the active mass surface.[39] Most notably, cells containing PFCHA moieties exhibited an additional semicircle in the range of 1 kHz – 1 Hz, which we hypothesize to be most likely caused by charge transfer in adsorbed ions on electrolyte/electrode interfaces. [40] The question whether these effects are specific to all-*cis*-fluorinated cyclohexane derivatives or if it can be exploited by more compounds with enhanced dielectric permittivity will be the subject of future work. [41].

Additionally, galvanostatic cycling with potential limitation (GCPL) was performed to evaluate the rate capabilities of both materials (refer to Fig. 3B). On the one hand, it was found that both materials exhibit satisfactory reversibility of capacity, especially poly(S-CHA-TEVS) was found to effectively recover from C–rates as aggressive as 3C back to its original capacities available at C/2 (100 %), C/5 (97 %), and C/10 (88 %). Poly(S-PFCHA-TEVS) on the other hand exhibited dramatically higher capacities but was slightly less effective in regaining its original capacity after cycling with 3C after which only 92 % of the capacity at C/2 were achievable. Further reduction of C-rate to C/5 and C/10 showed a capacity retention of 90 % and 88 % of the respective capacities that were reached before cycling at 3C. Charge-discharge profiles of poly(S-PFCHA-TEVS) and poly(S-CHA-TEVS) revealed that the voltage difference calculated from the charge–discharge plateau ($\Delta = 171$ mV) was lower for poly(S-PFCHA-TEVS) compared to that of poly(S-CHA-TEVS) ($\Delta = 183$ mV) resulting in lower electrochemical polarization (refer to Fig. 3C). This effect became more pronounced for increased C-rates, indicating a faster conversion of soluble lithium polysulfides to insoluble Li$_2$S$_2$/Li$_2$S in poly(S-PFCHA-TEVS).[39]

The self-discharge in Li-S batteries relies on diffusion of soluble polysulfides to the anode where they react with lithium to form insoluble Li$_2$S/Li$_2$S$_2$. This is associated with a gradual decay of potential between sulfur cathode and lithium anode. Thus, to substantiate the
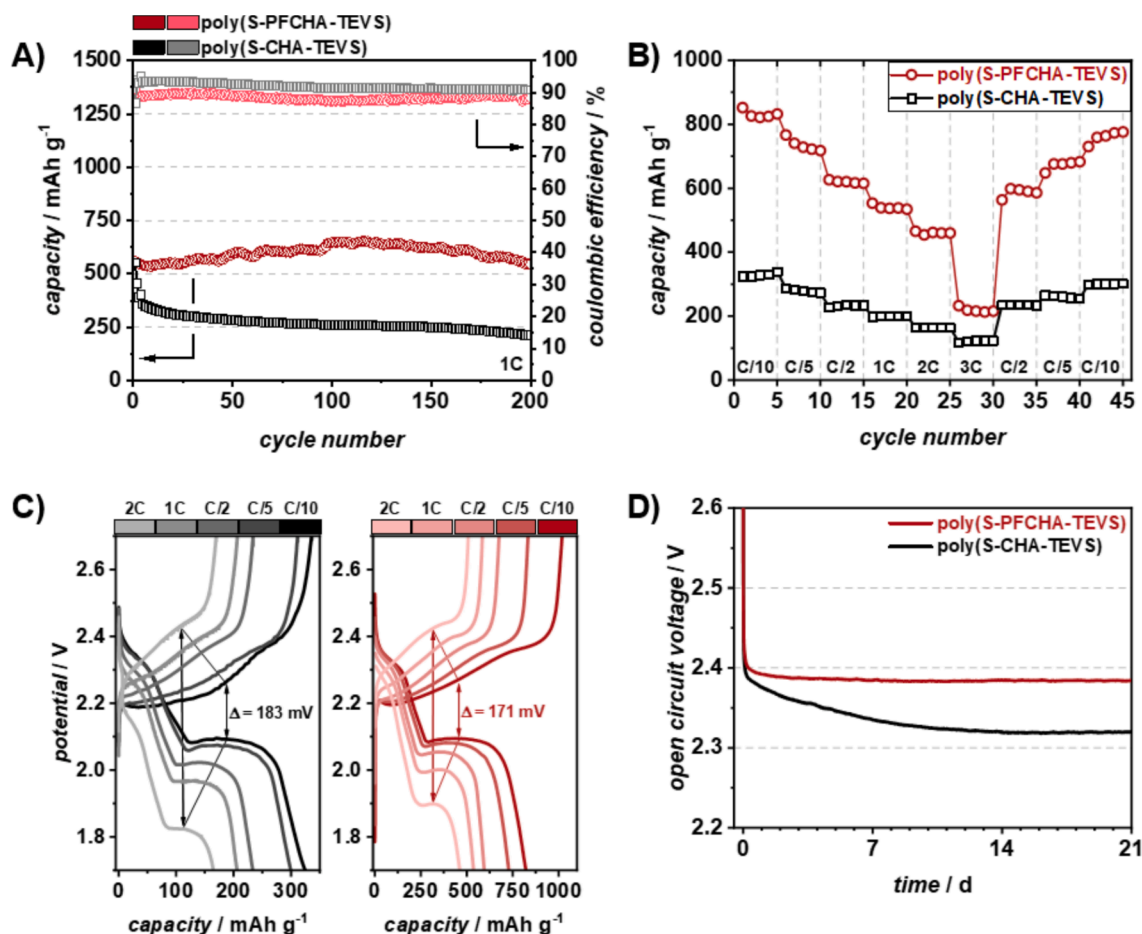
**Fig. 3.** Electrochemical charge–discharge analysis of Li-S cells with poly(S-PFCHA-TEVS) (red) and poly(S-CHA-TEVS) (black) cathode materials. A) Long term cycling at 1C. Poly(S-PFCHA-TEVS) cells show no significant capacity fading over 200 cycles while poly(S-CHA-TEVS) cells show constant capacity fading. B) GCPL and C) charge/discharge profiles at different C-rates. D) Comparison of the self-discharge of Li-S cells with poly(S-PFCHA-TEVS) and poly(S-CHA-TEVS), respectively. PFCHA-containing cells show almost no voltage fading after two initial discharge/charge cycles compared to CHA-containing cells.

hypothesis of inhibition of sulfide shuttling by introduction of all-*cis*-fluorinated cyclohexyl groups, the self-discharge of Li-S cells with poly (S-PFCHA-TEVS) and poly(S-CHA-TEVS) as cathode material were compared by monitoring the open circuit voltage over time. [42,43] Fresh cells were cycled at 0.2C for two cycles before the current was stopped, and the open circuit voltage was measured over time. Both cells showed a rapid drop in voltage after power was turned off. Interestingly, the poly(S-CHA-TEVS) cell showed a gradual decrease in voltage over a period of 14 days before reaching a plateau. Poly(S-PFCHA-TEVS) cells, on the other hand, showed almost no decay of voltage after the initial voltage drop for 21 days and therefore almost no self-discharge. The gradual voltage decay of cells with poly(S-PFCHA-TEVS) was as low as 20 mV after 21 days following the initial shut down while cells with poly (S-CHA-TEVS) lost 70 mV over the same time period. We conclude that the constant voltage is mainly caused by the inhibition of diffusion of polysulfide chains through the electrolyte due to their coordination to the high-polar all-*cis*-fluorinated cyclohexyl anchor points. [24,44].

## 2. Conclusion

In this work we presented the synthesis and IV of all-*cis*-2,3,4,5,6-pentafluorocyclohexyl acrylate for the first time. The obtained material was employed as cathode material in Li-S cells and compared to its non-fluorinated analogue. The cell performance of the PFCHA-containing material was found to be significantly enhanced in comparison to the non-fluorinated reference material, which was concluded from superior lithium-ion diffusion evaluated by CV analysis. Cycling experiments

revealed a capacity retention of 98 % after 200 cycles at 1C and 96 % after 200 cycles at 0.5C before capacity fading. The comparative reference material exhibited a capacity retention of 38 % and 61 % after 200 cycles, respectively. Investigation of self-discharge showed a voltage decay of 20 mV over 21 days in PFCHA-containing Li-S cells (compared to 70 mV) and we suggest that the presence of highly polar moieties in PFCHA leads to inhibition of sulfide-shuttling, but can currently not rule out other explanations such as generally improved dielectric permittivity caused by PFCHA. Further studies are necessary to gain deeper understanding of the exact structural features and coordination behavior of polysulfides at Janus-faced moieties in Li-S batteries which we believe will broaden the applicability of such compounds in modern energy storage systems. Nevertheless, the synthetic strategy presented herein represents itself a very promising approach for the development of novel high-performance energy storage systems based on all-*cis*-fluorinated compounds.

Data availability statement.

Author Contributions.

A. P. G., M. v. D., and P. T. proposed the original idea (equal). A. P. G. designed, synthesized, and characterized the polymer, curated, and analyzed the data, and wrote the original draft (lead). B. D. built the cells, assisted with electrochemical characterization. S. V. H. synthesized and characterized PFCHA (lead). D. V. and C. W. S. administrated the project and validated the data. M. v. D., F. S., and P. T. acquired

funding and supervised the project (lead). B. D., S. V. H., D. V., C. W. S., M. v. D., F. S., and P. T. corrected the paper (equal).

## CRediT authorship contribution statement

**Alexander P. Grimm:** Writing – original draft, Visualization, Validation, Methodology, Investigation, Formal analysis, Data curation. **Bijian Deng:** Writing – original draft, Validation, Methodology, Investigation, Formal analysis, Data curation. **Shyamkumar V. Haridas:** Writing – original draft, Validation, Methodology, Investigation, Formal analysis. **Dominik Voll:** Writing – original draft, Supervision, Project administration. **Christian W. Schmitt:** Writing – original draft, Supervision, Project administration. **Max von Delius:** Writing – review & editing, Validation, Supervision, Project administration, Funding acquisition, Conceptualization. **Frieder Scheiba:** Writing – review & editing, Validation, Supervision, Project administration, Funding acquisition. **Patrick Théato:** Writing – review & editing, Validation, Supervision, Project administration, Funding acquisition, Conceptualization.

## Declaration of competing interest

The authors declare that they have no known competing financial interests or personal relationships that could have appeared to influence the work reported in this paper.

## Acknowledgement

## Appendix A. Supplementary data

Supplementary data to this article can be found online at https://doi.org/10.1016/j.eurpolymj.2025.113815.

## Data availability

Raw data sets can be found in the RADAR4Chem Repository under the following digital object identifier: 10.22000/4bh51mv09m2hr1b2

## References

[1] T. Lee, P.T. Dirlam, J.T. Njardarson, R.S. Glass, J. Pyun, Polymerizations with Elemental Sulfur: From Petroleum Refining to Polymeric Materials, J. Am. Chem. Soc. 144 (2022) 5–22, https://doi.org/10.1021/jacs.1c09329.

[2] J.J. Griebel, R.S. Glass, K. Char, J. Pyun, Polymerizations with elemental sulfur: A novel route to high sulfur content polymers for sustainability, energy and defense, Prog. Polym. Sci. 58 (2016) 90–125, https://doi.org/10.1016/j.progpolymsci.2016.04.003.

[3] H. Mutlu, E.B. Ceper, X. Li, J. Yang, W. Dong, M.M. Ozmen, P. Theato, Sulfur Chemistry in Polymer and Materials Science, Macromol. Rapid Commun. 40 (2019) e1800650, https://doi.org/10.1002/marc.201800650.

[4] W.J. Chung, J.J. Griebel, E.T. Kim, H. Yoon, A.G. Simmonds, H.J. Ji, P.T. Dirlam, R. S. Glass, J.J. Wie, N.A. Nguyen, B.W. Guralnick, J. Park, A. Somogyi, P. Theato, M. E. Mackay, Y.-E. Sung, K. Char, J. Pyun, The use of elemental sulfur as an alternative feedstock for polymeric materials, Nat. Chem. 5 (2013) 518–524, https://doi.org/10.1038/nchem.1624.

[5] J.M. Chalker, M.J.H. Worthington, N.A. Lundquist, L.J. Esdaile, Synthesis and Applications of Polymers Made by Inverse Vulcanization, Top. Curr. Chem. (cham) 377 (2019) 16, https://doi.org/10.1007/s41061-019-0242-7.

[6] M.P. Crockett, A.M. Evans, M.J.H. Worthington, I.S. Albuquerque, A.D. Slattery, C. T. Gibson, J.A. Campbell, D.A. Lewis, G.J.L. Bernardes, J.M. Chalker, Sulfur-Limonene Polysulfide: A Material Synthesized Entirely from Industrial By-Products

[7] and Its Use in Removing Toxic Metals from Water and Soil, Angew. Chem. Int. Ed. 55 (2016) 1714–1718, https://doi.org/10.1002/anie.201508708.

[7] A.P. Grimm, M. Plank, A. Stihl, C.W. Schmitt, D. Voll, F.H. Schacher, J. Lahann, P. Theato, Inverse Vulcanization of Activated Norbornenyl Esters – A Versatile Platform for Functional Sulfur Polymers, Angew. Chem. Int. Ed. e202411010 (2024), https://doi.org/10.1002/anie.202411010.

[8] J.J. Griebel, S. Namnabat, E.T. Kim, R. Himmelhuber, D.H. Moronta, W.J. Chung, A.G. Simmonds, K.-J. Kim, J. van der Laan, N.A. Nguyen, E.L. Dereniak, M. E. Mackay, K. Char, R.S. Glass, R.A. Norwood, J. Pyun, New infrared transmitting material via inverse vulcanization of elemental sulfur to prepare high refractive index polymers, Adv. Mater. 26 (2014) 3014–3018, https://doi.org/10.1002/adma.201305607.

[9] J. Molineux, T. Lee, K.J. Kim, K.-S. Kang, N.P. Lyons, A. Nishant, T.S. Kleine, S. W. Durfee, J. Pyun, R.A. Norwood, Fabrication of Plastic Optics from Chalcogenide Hybrid Inorganic/Organic Polymers for Infrared Thermal Imaging, Adv. Opt. Mat. 12 (2024) 2301971, https://doi.org/10.1002/adom.202301971.

[10] J.A. Smith, R. Mulhall, S. Goodman, G. Fleming, H. Allison, R. Raval, T. Hasell, Investigating the Antibacterial Properties of Inverse Vulcanized Sulfur Polymers, ACS Omega 5 (2020) 5229–5234, https://doi.org/10.1021/acsomega.9b04267.

[11] V.S. Wadi, K.K. Jena, S.Z. Khawaja, V.M. Ranagraj, S.M. Alhassan, Preparation and processing of porous sulfur foams having low thermal conductivity, RSC Adv. 9 (2019) 4397–4403, https://doi.org/10.1039/c8ra09127g.

[12] A.S.M. Ghumman, R. Shamsuddin, R. Sabir, A. Waheed, A. Sami, H. Almohamadi, Synthesis and performance evaluation of slow-release fertilizers produced from inverse vulcanized copolymers obtained from industrial waste, RSC Adv. 13 (2023) 7867–7876, https://doi.org/10.1039/d3ra00256j.

[13] S.F. Valle, A.S. Giroto, R. Klaic, G.G. Guimarães, C. Ribeiro, Sulfur fertilizer based on inverse vulcanization process with soybean oil, Polym. Degrad. Stab. 162 (2019) 102–105, https://doi.org/10.1016/j.polymdegradstab.2019.02.011.

[14] S.J. Tonkin, C.T. Gibson, J.A. Campbell, D.A. Lewis, A. Karton, T. Hasell, J. M. Chalker, Chemically induced repair, adhesion, and recycling of polymers made by inverse vulcanization, Chem. Sci. 11 (2020) 5537–5546, https://doi.org/10.1039/d0sc00855a.

[15] N.A. Lundquist, A.D. Tikoalu, M.J.H. Worthington, R. Shapter, S.J. Tonkin, F. Stojcevski, M. Mann, C.T. Gibson, J.R. Gascooke, A. Karton, L.C. Henderson, L. J. Esdaile, J.M. Chalker, Reactive Compression Molding Post-Inverse Vulcanization: A Method to Assemble, Recycle, and Repurpose Sulfur Polymers and Composites, Chemistry 26 (2020) 10035–10044, https://doi.org/10.1002/chem.202001841.

[16] P.T. Dirlam, A.G. Simmonds, T.S. Kleine, N.A. Nguyen, L.E. Anderson, A.O. Klever, A. Florian, P.J. Costanzo, P. Theato, M.E. Mackay, R.S. Glass, K. Char, J. Pyun, Inverse vulcanization of elemental sulfur with 1,4-diphenylbutadiyne for cathode materials in Li–S batteries, RSC Adv. 5 (2015) 24718–24722, https://doi.org/10.1039/C5RA01188D.

[17] H. Wang, B. Zhang, R. Dop, P. Yan, A.R. Neale, L.J. Hardwick, T. Hasell, Oxygen heteroatom enhanced sulfur-rich polymers synthesized by inverse vulcanization for high-performance lithium-sulfur batteries, J. Power Sources 545 (2022) 231921, https://doi.org/10.1016/j.jpowsour.2022.231921.

[18] H. Li, Y. Li, L. Zhang, Designing principles of advanced sulfur cathodes toward practical lithium-sulfur batteries, SusMat 2 (2022) 34–64, https://doi.org/10.1002/sus2.42.

[19] M. Wang, Z. Bai, T. Yang, C. Nie, X. Xu, Y. Wang, J. Yang, S. Dou, N. Wang, Advances in High Sulfur Loading Cathodes for Practical Lithium-Sulfur Batteries, Adv. Energy Mater. (2022) 2201585, https://doi.org/10.1002/aenm.202201585.

[20] R. Zou, W. Liu, F. Ran, Sulfur-containing polymer cathode materials: From energy storage mechanism to energy density, InfoMat 4 (2022) e12319, https://doi.org/10.1002/inf2.12319.

[21] D. O'Hagan, Polar Organofluorine Substituents: Multivicinal Fluorines on Alkyl Chains and Alicyclic Rings, Chemistry 26 (2020) 7981–7997, https://doi.org/10.1002/chem.202000178.

[22] D. O'Hagan, The Emergence and Properties of Selectively Fluorinated 'Janus' Cyclohexanes, Chem. Rec. 23 (2023) e202300027, https://doi.org/10.1002/tcr.202300027.

[23] N.S. Keddie, A.M.Z. Slawin, T. Lebl, D. Philp, D. O'Hagan, All-cis 1,2,3,4,5,6-hexafluorocyclohexane is a facially polarized cyclohexane, Nat. Chem. 7 (2015) 483–488, https://doi.org/10.1038/nchem.2232.

[24] O. Shyshov, K.A. Siewerth, M. von Delius, Evidence for anion-binding of all-cis hexafluorocyclohexane in solution and solid state, Chem. Commun. 54 (2018) 4353–4355, https://doi.org/10.1039/c8cc01797b.

[25] J.L. Clark, R.M. Neyyappadath, C. Yu, A.M.Z. Slawin, D.B. Cordes, D. O'Hagan, Janus All-Cis 2,3,4,5,6-Pentafluorocyclohexyl Building Blocks Applied to Medicinal Chemistry and Bioactives Discovery Chemistry, Chemistry 27 (2021) 16000–16005, https://doi.org/10.1002/chem.202102819.

[26] N. Al-Maharik, P. Kirsch, A.M.Z. Slawin, D.B. Cordes, D. O'Hagan, Fluorinated liquid crystals: evaluation of selectively fluorinated facially polarised cyclohexyl motifs for liquid crystal applications, Org. Biomol. Chem. 14 (2016) 9974–9980, https://doi.org/10.1039/c6ob01986b.

[27] S.V. Haridas, M. von Delius, Synthesis and supramolecular properties of all-cis-2,4,6-trifluorocyclohexane-1,3,5-triol, Chem. Commun. 60 (2024) 606–609, https://doi.org/10.1039/d3cc05510h.

[28] O. Shyshov, S.V. Haridas, L. Pesce, H. Qi, A. Gardin, D. Bochicchio, U. Kaiser, G. M. Pavan, M. von Delius, Living supramolecular polymerization of fluorinated cyclohexanes, Nat. Commun. 12 (2021) 3134, https://doi.org/10.1038/s41467-021-23370-y.

[29] S.V. Haridas, O. Shyshov, M. von Delius, Supramolecular Polymerization of all-cis-Fluorinated Cyclohexanes: Influence of Side Chains, Org. Mater. 5 (2023) 166–174, https://doi.org/10.1055/s-0043-1761314.

[30] M.P. Wiesenfeldt, Z. Nairoukh, W. Li, F. Glorius, Hydrogenation of fluoroarenes: Direct access to all-cis-(multi)fluorinated cycloalkanes, Science 357 (2017) 908–912, https://doi.org/10.1126/science.aao0270.

[31] S.M. Pratik, A. Nijamudheen, A. Datta, Janus all-cis-1,2,3,4,5,6-Hexafluorocyclohexane: A Molecular Motif for Aggregation-Induced Enhanced Polarization, ChemPhysChem 17 (2016) 2373–2381, https://doi.org/10.1002/cphc.201600262.

[32] F. Yan, J. Jiang, X. Chen, S. Tian, K. Li, Synthesis and Characterization of Silica Nanoparticles Preparing by Low-Temperature Vapor-Phase Hydrolysis of SiCl 4, Ind. Eng. Chem. Res. 53 (2014) 11884–11890, https://doi.org/10.1021/ie501759w.

[33] A.P. Grimm, J.M. Scheiger, P.W. Roesky, P. Théato, Inverse vulcanization of trimethoxyvinylsilane particles, Polym. Chem. (2022), https://doi.org/10.1039/D2PY00773H.

[34] S.S. Zhang, Liquid electrolyte lithium/sulfur battery: Fundamental chemistry, problems, and solutions, J. Power Sources 231 (2013) 153–162, https://doi.org/10.1016/j.jpowsour.2012.12.102.

[35] A. Hoefling, D.T. Nguyen, Y.J. Lee, S.-W. Song, P. Theato, A sulfur–eugenol allyl ether copolymer: a material synthesized via inverse vulcanization from renewable resources and its application in Li–S batteries, Mater. Chem. Front. 1 (2017) 1818–1822, https://doi.org/10.1039/C7QM00083A.

[36] H.-L. Wu, L.A. Huff, A.A. Gewirth, In situ Raman spectroscopy of sulfur speciation in lithium-sulfur batteries, ACS Appl. Mater. Interfaces 7 (2015) 1709–1719, https://doi.org/10.1021/am5072942.

[37] M. Liu, Z. Wu, S. Liu, T. Guo, P. Chen, X. Cao, S. Pan, T. Zhou, L. Pompizii, M. Najafov, A. Coskun, Y. Fu, Accelerated Reversible Conversion of Li2S2 to Li2S

[38] by Spidroin Regulated Li+ Flux for High-performance Li-Sulfur Batteries, Angew. Chem. Int. Ed. (2024) e202417624, https://doi.org/10.1002/anie.202417624.

[38] L. Liu, Y. Meng, Y. Ge, D. Xiao, Regulating Polysulfide Transformation and Deposition Kinetics in Lithium-Sulfur Batteries Based on 3D Conductive Framework, ACS Appl. Mater. Interfaces (2023), https://doi.org/10.1021/acsami.3c03801.

[39] L. Li, J.S. Nam, M.S. Kim, Y. Wang, S. Jiang, H. Hou, I.-D. Kim, Sulfur–Carbon Electrode with PEO-LiFSI-PVDF Composite Coating for High-Rate and Long-Life Lithium–Sulfur Batteries, Adv. Energy Mater. 13 (2023) 2302139, https://doi.org/10.1002/aenm.202302139.

[40] R. Tatara, P. Karayaylali, Y. Yu, Y. Zhang, L. Giordano, F. Maglia, R. Jung, J. P. Schmidt, I. Lund, Y. Shao-Horn, The Effect of Electrode-Electrolyte Interface on the Electrochemical Impedance Spectra for Positive Electrode in Li-Ion Battery, J. Electrochem. Soc. 166 (2019) A5090–A5098, https://doi.org/10.1149/2.0121903jes.

[41] A. Theodoridis, G. Papamokos, M.P. Wiesenfeldt, M. Wollenburg, K. Müllen, F. Glorius, G. Floudas, Polarity Matters: Dielectric Relaxation in All-cis-Multifluorinated Cycloalkanes, J. Phys. Chem. B 125 (2021) 3700–3709, https://doi.org/10.1021/acs.jpcb.1c00100.

[42] G. Wen, S. Rehman, T.G. Tranter, D. Ghosh, Z. Chen, J.T. Gostick, M.A. Pope, Insights into Multiphase Reactions during Self-Discharge of Li-S Batteries, Chem. Mater. 32 (2020) 4518–4526, https://doi.org/10.1021/acs.chemmater.0c00235.

[43] C. Shen, J. Xie, M. Zhang, P. Andrei, M. Hendrickson, E.J. Plichta, J.P. Zheng, Self-Discharge Behavior of Lithium-Sulfur Batteries at Different Electrolyte/Sulfur Ratios, J. Electrochem. Soc. 166 (2019) A5287–A5294, https://doi.org/10.1149/2.0461903jes.

[44] Z. Zeng, X. Liu, Sulfur Immobilization by "Chemical Anchor" to Suppress the Diffusion of Polysulfides in Lithium–Sulfur Batteries, Adv. Mater. Interfaces 5 (2018) 1701274, https://doi.org/10.1002/admi.201701274.